Absence of exchange interaction between localized magnetic moments and conduction-electrons in diluted Er^{3+} gold-nanoparticles

G. G. Lesseux,[1,a)] W. Iwamoto,[1,2] A. F. García-Flores,[3] R. R. Urbano,[1] and C. Rettori[1,3]
[1]*Instituto de Física "Gleb Wataghin," UNICAMP, 13083-859 Campinas, São Paulo, Brazil*
[2]*Instituto de Física, UFU, 38400-902 Uberlândia, Minas Gerais, Brazil*
[3]*Centro de Ciências Naturais e Humanas, UFABC, 09210-971 Santo André, São Paulo, Brazil*

(Presented 5 November 2013; received 23 September 2013; accepted 25 November 2013; published online 28 February 2014)

The Electron Spin Resonance (ESR) of diluted Er^{3+} magnetic ions in Au nanoparticles (NPs) is reported. The NPs were synthesized by reducing chloro triphenyl-phosphine gold(I) and erbium(III) trifluoroacetate. The Er^{3+} g-value along with the observed hyperfine splitting indicate that the Er^{3+} impurities are in a local cubic symmetry. Furthermore, the Er^{3+} ESR spectra show that the exchange interaction between the $4f$ and the conduction electrons (ce) is absent or negligible in $Au_{1-x}Er_x$ NPs, in contrast to the ESR results in bulk $Au_{1-x}Er_x$. Therefore, the nature of this interaction needs to be reexamined at the nano scale range. © *2014 AIP Publishing LLC*. [http://dx.doi.org/10.1063/1.4867126]

I. INTRODUCTION

Gold nanoparticles (Au NPs) have become a subject of increasing scientific and technological interest in the last two decades. Properties such as catalytic activity,[1] biological compatibility,[2] and unexpected magnetic polarization[3] are some examples of the motivation to study Au NPs. In this work, we present a chemical route to obtain $Au_{1-x}Er_x$ NPs and report T-dependent Electron Spin Resonance (ESR) experiments in these NPs and in their bulk version. Our results indicate that the exchange interaction between the spin of the localized magnetic moments and the spin of the conduction electrons (ce) is absent in $Au_{1-x}Er_x$ NPs.

II. EXPERIMENTAL DETAIL

The diluted alloy of $Au_{1-x}Er_x$, labelled as bulk, was prepared by arc-melting the appropriated stoichiometric amounts of elements under inert argon atmosphere.[4]

The diluted Er^{3+} gold-nanoparticles were synthesized by a chemical route adapting the procedure for silver NPs described by Tang *et al.*[5,6] This route consists in the reduction of two precursor compounds. Needle type crystals of Chloro(triphenylphosphine)gold(I) were used as Au-metallic precursor. The rare-earth precursor, $Er(CF_3COO)_3$, was obtained by a method described by J. E. Roberts.[7] The appropriated molar proportion of the two precursors were dissolved in 20 ml benzyl ether. Oleylamine (5 ml) and oleic acid (5 ml) were added to act as stabilizers. The solution was heated up to 100 °C and maintained at this temperature for 30 min with vigorous stirring under argon flow to dehydration. Thereafter, heating was increased to 200 °C under reflux, and 2 ml of a 1M tetrahydrofuran (THF) solution of lithium triethylborohydride reductor was added to the solution. The temperature was then increased to 250 °C for 30 min under argon flow. Finally, the solution was cooled down to room-T and centrifuged after adding excess of ethanol. The nanoparticles can be easily dispersed in nonpolar solvents such as toluene.

The size and shape of the sample was analyzed in a SEM (FEI Inspect F50), and the structure was checked out by X-ray powder diffraction (XRD) using the Cu-K_α radiation in a Phillips Diffractometer at room-T. The magnetic properties were characterized by means of magnetization measurements as a function of temperature between 300 K and 2 K using a superconducting quantum interference device (SQUID) magnetometer MPMS-5 (Quantum Design). The ESR experiments, between 4.2 K and 300 K, were carried out in a Bruker ELEXYS-500 X-Band (9.5 GHz) spectrometer with a TE_{102} resonator coupled to a cool helium gas flow cryostat and an Oxford T-controller.

III. RESULTS AND DISCUSSION

Figure 1 presents the XRD pattern for the $Au_{1-x}Er_x$ NPs which was indexed on the basis of the face-centered-cubic (fcc) Au XRD data. The inset on the left hand side of Fig. 1 shows the {200} peak. This and the peaks {111} and {220} were duplicated. The inset on the right hand side of Fig. 1 shows the SEM image of $Au_{1-x}Er_x$ NPs presenting two different morphological phases: Cubic-like F1 (edges of 66 nm) and spherical-like F2 (≈35 nm in diameter) shapes. This is probably the reason for duplicated peaks. The line width values of the pseudo-Voigt adjustments of these peaks and the Scherrer's formula[8] were used to estimate the average size of the NPs. The estimated size values were 75(9) nm for F1 and 32(2) nm for F2. These values are in reasonably agreement with the SEM image.

The T-dependence of the magnetic susceptibility for the $Au_{1-x}Er_x$ NPs is shown in Fig. 2. The Curie–Weiss behavior of the susceptibility indicates that the paramagnetic signal is due to weak-interacting localized magnetic moments. The inverse of the paramagnetic susceptibility was fitted between 120 K and 270 K by the Curie–Weiss law, assuming that the

a)Electronic mail: lesseux@ifi.unicamp.br

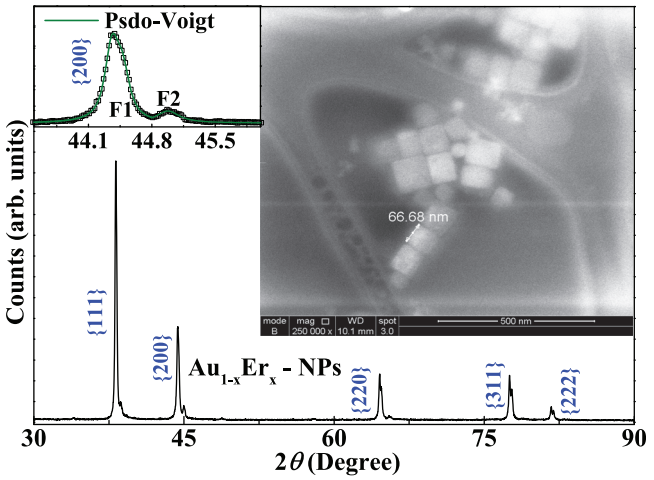

FIG. 1. X-Ray powder diffraction pattern for $Au_{1-x}Er_x$ NPs. The inset on the left hand side shows the pseudo-Voigt function fit for the cubic {200} peaks. The inset on the right hand side shows the SEM image of $Au_{1-x}Er_x$ NPs.

magnetic moment corresponds to that of Er^{3+} ions. From the best fit, we obtained a Er^{3+} concentration of $\approx 1\%$.

Figure 3 shows the Er^{3+} X-band ESR spectra at 4.2 K for both NPs and bulk samples. The difference between the spectra is noteworthy. The spectrum of the bulk sample shows a typical Dysonian line-shape (skin depth $\ll$ particle size)[9] with the expected resolved hyperfine structure for bulk $Au_{1-x}Er_x$ alloy with $x \approx 0.07\%$.[10] The g-value of ≈ 6.77 is almost T-independent between 4.2 K and 25 K (see Fig. 4(a)), and the T-dependence of the Er^{3+} ESR intensity follows approximately a Curie–Weiss law (see Fig. 4(c)). These results confirm that the Er^{3+} ESR arises from a Γ_7 Kramers doublet ground state of the cubic crystalline electrical field (CEF) splitted J-multiplet ($J = 15/2$), in agreement with previous results for bulk $Au_{1-x}Er_x$ alloys.[4] Nonetheless, the Er^{3+} ESR of the NPs (see Fig. 3) presents a Lorentzian line-shape (skin depth $\gg$ particle size)[9] and resolved hyperfine structure corresponding to the ^{167}Er ($I = 7/2$) isotope. The obtained hyperfine parameter $^{167}A = 74(1)$ Oe is in good agreement with the value reported for low concentrated

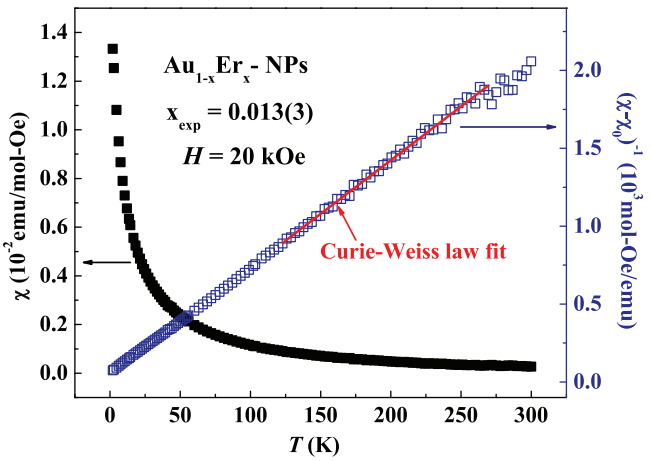

FIG. 2. T-dependence of the magnetic susceptibility (black square) and its inverse (open dark blue square) between 2 K and 300 K for $Au_{1-x}Er_x$ NPs. The solid red line is the fit to the inverse of the Curie–Weiss law.

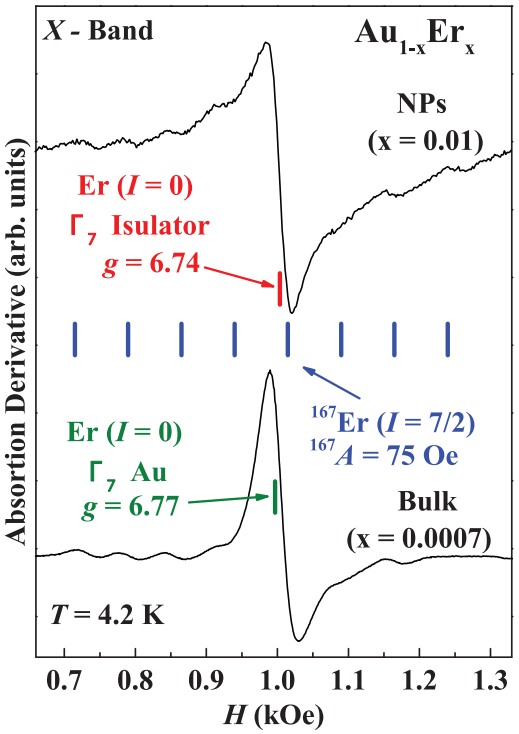

FIG. 3. Er^{3+} X-band ESR spectra of Au NPs and bulk at $T = 4.2$ K. The expected g-values for Er^{3+} in a Γ_7 Kramers doublet ground state in an insulator (red vertical line) and in gold (green vertical line) are shown. The vertical blue lines indicate the positions of the various hyperfine lines of the ^{167}Er ($I = 7/2$) isotope.

$Au_{1-x}Er_x$ bulk alloys.[10] The almost T-independent $g \approx 6.75$ between 4.2 K and 45 K and the Curie–Weiss-like behavior of the ESR intensity for the NPs (see Figs. 4(a) and 4(c)) lead us to conclude that the Er^{3+} ions are at the cubic sites in the $Au_{1-x}Er_x$ NPs with a Γ_7 Kramers doublet ground state.

Figures 4(a) and 4(b) show the T-dependence of the g-value and linewidth, $\Delta H_{eff} \equiv \Delta H - \Delta H_0$, after subtracting the residual linewidth, $\Delta H_0 (\Delta H_0 = \Delta H(T \to 0))$, at X-band ($\nu \approx 9.5$ GHz) for the NPs and bulk $Au_{1-x}Er_x$ samples. The T-independent g-value of ≈ 6.75 for the NPs is close to the Γ_7 g-value reported for Er^{3+} in the cubic insulating ThO_2 host.[11] Thus, within the accuracy of our ESR experiments, the g-value in our $Au_{1-x}Er_x$ NPs does not show the g-shift observed for bulk $Au_{1-x}Er_x$ which is attributed to the exchange interaction between the Er^{3+} localized spin **S** and *ce* ones **s**, $J_{fs}\mathbf{S} \cdot \mathbf{s}$.[10] This result suggests that this exchange interaction is absent or negligible in our $Au_{1-x}Er_x$ NPs.

The low-T ΔH_{eff}, in bulk $Au_{1-x}Er_x$, follows a linear behavior, $\Delta H_{eff} = bT$, known as Korringa-relaxation.[12] This provides a Korringa ratio $b = 2.5(1)$ Oe/K. Above $T \approx 7$ K, there is an exponential broadening. Assuming that the latter broadening is associated to the spin-lattice relaxation via exchange interaction with the *ce* involving excited CEF levels, an appropriately fitting[13] of ΔH_{eff} (see Fig. 4(b)) leads to a value of $\Delta = 28(3)$ K for the energy splitting between the first excited CEF level and the ground state. For the NPs, ΔH_{eff} is constant at low-T, i.e., the Korringa-relaxation is absent, and there is an exponential broadening above $T \approx 16$ K. Therefore, due to the absence of exchange interaction with the *ce*, the line broadening must be associated with

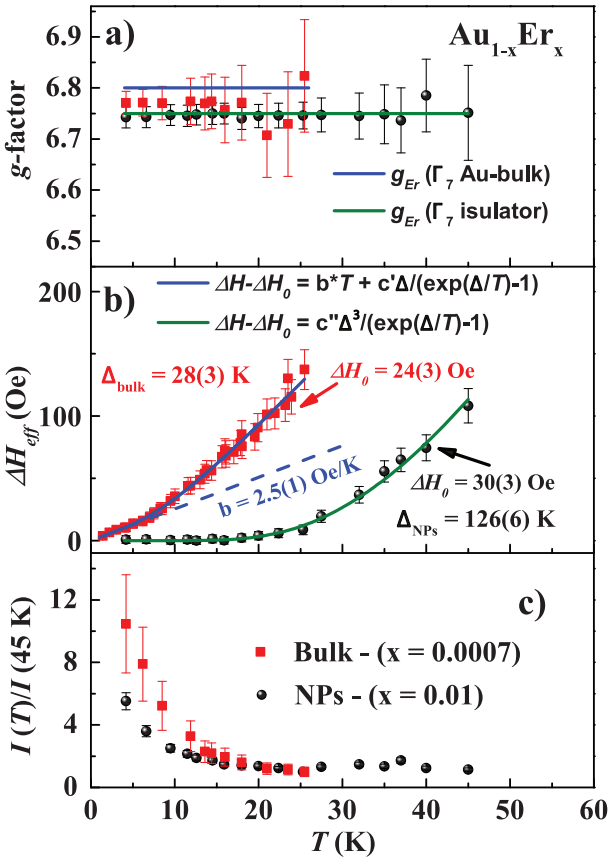

FIG. 4. T-dependence of (a) g-value, (b) ΔH_{eff} ($\equiv \Delta H - \Delta H_0$), (c) normalized integrated ESR intensity for Er^{3+} in Au Nps (black spheres) and bulk (red squares). The solid lines show (a) the g-value for Er^{3+} in a Γ_7 Kramers doublet ground state in insulators (green) and in gold (blue) and (b) fits of the T-dependence of ΔH_{eff} for NPs (green) and bulk (blue).

a spin-lattice relaxation via the two phonon Orbach process involving excited CEF levels. An appropriate fitting[13] of ΔH_{eff} (see Fig. 4(b)) leads to a value of $\Delta = 126(6)$ K for the CEF splitting. Thus, these results indicate that, besides the absence of g-shift and Korringa-relaxation, the effective strength of the cubic CEF at the Er^{3+} site was strongly affected by the finite size of the NPs.

IV. CONCLUSIONS

In summary, our results provide strong experimental evidences for the existence of finite size effects on some of the ground state properties of the Er^{3+} diluted Au NPs. The local field (absence of g-shift), the spin-lattice relaxation (absence of Korringa-relaxation), and the strength of the cubic CEF were dramatically affected. These results suggest that the effect of the exchange interaction between localized magnetic moments and the *ce*, $J_{fs}\mathbf{S}\cdot\mathbf{s}$, was suppressed, and the intensity of the cubic CEF strongly enhanced in the NPs. We suggest that the absence of exchange interaction with the *ce* may be due to the onset of *ce* localization in the NPs (discrete density of state at the Fermi level), i.e., quantum size effects may start to be observable in our ESR measurements already at NPs size of 30 to 60 nm. The increase of the cubic CEF splitting may be associated with changes in the lattice parameters which are related to different morphology (size and shape) of the $Au_{1-x}Er_x$ NPs if compared to the bulk form.[14] Besides, a subtle interplay between the boundary conditions and the presence of crystalline defects, imposed by the finite size of the NPs, may strongly perturbate the *ce* of the Au host and, in turn, affect the static and dynamic properties of the localized magnetic moment ground state in these $Au_{1-x}Er_x$ NPs.[6]

ACKNOWLEDGMENTS

This work was supported by Fapesp, CAPES, and CNPq-Brazil. The SEM (FEI Inspect F50) experiment was carried out at the Brazilian Nanotechnology National Laboratory (LNNano).

[1]M. Daniel and D. Astruc, Chem. Rev. **104**, 293 (2004).
[2]R. Shukla, V. Bansal, M. Chaudhary, A. Basu, R. R. Bhonde, and M. Sastry, Langmuir **21**, 10644 (2005).
[3]S. Trudel, Gold Bull. **44**, 3 (2011).
[4]C. Rettori, D. Davidov, and H. M. Kim, Phys. Rev. B **8**, 5335 (1973).
[5]Y. Tang and M. Ouyang, Nature Mater. **6**, 754 (2007).
[6]J. M. Vargas, W. Iwamoto, L. M. Holanda, S. B. Oseroff, P. G. Pagliuso, and C. Rettori, J. Nanosci. Nanotechnol. **11**, 2126 (2011).
[7]J. E. Roberts, J. Am. Chem. Soc. **83**, 1087 (1961).
[8]B. D. Cullity and S. R. Stock, *Elements of X-Ray Diffraction*, 3rd ed. (Prentice-Hall Inc., 2001), pp. 170.
[9]G. Feher and A. F. Kip, Phys. Rev. **98**, 337 (1955); F. J. Dyson, *ibid.* **98**, 349 (1955).
[10]L. J. Tao, D. Davidov, R. Orbach, and E. P. Chock, Phys. Rev. B **4**, 5 (1971).
[11]A. Abraham, R. A. Weeks, G. W. Clark, and C. B. Finch, Phys. Rev. **137**, A138 (1965).
[12]J. Korringa, Physica **16**, 601 (1950).
[13]D. Davidov, C. Rettori, A. Dixon, K. Baberschke, E. P. Chock, and R. Orbach, Phys. Rev. B **8**, 3563 (1973).
[14]W. Qi and M. Wang, J. Nanopart. Res. **7**, 51 (2005).